Self-Propagating High-Temperature Synthesis of Intermetallic Compounds: A Computer Simulation Approach to the Chemical Mechanisms

Silvia Gennari, Filippo Maglia,* Umberto Anselmi-Tamburini, and Giorgio Spinolo

INSTM, IENI/CNR, and Department Physical Chemistry, University of Pavia, Viale Taramelli, 16, I 27100 Pavia Italy

Received: August 7, 2002; In Final Form: November 15, 2002

The self-propagating high-temperature reaction in nickel−aluminum powder mixtures has been investigated by computer simulated experiments using a monodimensional model. The model describes the overall reaction mechanism considering several elemental steps such as melting of the reactant Al, diffusion-controlled dissolution of solid nickel into the molten pool, (possible) melting of the Ni reactant, precipitation and melting of the compound, and precipitation of the eutectic mixture of Al + AlNi. Melting of pure aluminum and nickel and eutectic crystallization are considered in terms of thermal balance only, whereas an explicit diffusion controlled kinetic for the dissolution of nickel in molten aluminum was accounted for. The results show that the reaction propagates under almost steady conditions with constant wave velocity and peak temperature, close to experimentally reported values, when suitable values for the thermal conductivity of the green compact were set.

1. Introduction

Thanks to its numerous attractive characteristics, self-propagating high-temperature synthesis (SHS, also known as combustion synthesis) has been employed in the last thirty years to synthesize a large number of inorganic materials.[1−3] Among them, intermetallic compounds and, in particular, transition metal aluminides have been produced by SHS since the early 1970s, and numerous experimental investigations are nowadays available. Interest for the SHS route is due both to its generic advantages as a tool for high-temperature synthesis (low cost, simplicity of the apparatus, fast process) and to specific properties of the products related to many applications such as high-temperature structural materials, hydrogen storage, and thermoelectric devices.[4]

Among the Al-based intermetallic compounds, the SHS in the Al−Ni system has been studied by several different approaches,[5] including related techniques (such as combustion on thin foils, and thermal explosion methods) and is, to our knowledge, one of the few examples in which the SHS mechanism has been investigated in great detail. In contrast to the conventional gas combustion processes, SHS nearly always involves heterogeneous reactions and the corresponding mechanism has the complexity of condensed phase reactions. Therefore, the experimental investigations of the chemical mechanisms of SHS reactions still represent a challenging task because of the lack of powerful direct investigation methods. Indeed, very generic mechanistic insights are provided by phase and composition analysis and by microscopic observation of the samples at the end of the process, or after a thermal quenching, whereas only indirect information is given by monitoring profile and velocity of the combustion wave with videorecording or with more specific pyrometric methods.[6] Time-resolved diffraction gives the most reliable mechanistic information but can be hardly used in routine work.[7−9]

In their study on the synthesis of the AlNi compound, Naiborodenko and Itin[10−12] reported as the SHS reaction can proceed through three different routes depending on the combustion temperature which, in turn, is related to the stoichiometry of the reacting mixture and/or the dilution degree. A first mechanism is active when the combustion temperature is below the melting point of the desired product but above the melting point of the reactants and all intermediate phases (Al_3Ni_2 and Al_3Ni). A second one is active when the temperature is below the melting points of Ni and AlNi but above the melting point of Al and the other intermediate phases. The third reported mechanism is active when the temperature is lowered below the melting point of one or several intermediate phases. In each of the possible mechanisms, different rate-limiting steps are active. In particular when the first route is active, diffusion of nickel in the molten aluminum is the rate controlling process, and an activation energy of 17.9 ± 2.9 kcal/mol was reported.[11] The corresponding combustion regime was reported by the same authors to be stationary or weakly oscillating.

Recently Fan et al.,[5] using the combustion front quenching method, experimentally investigated the reaction mechanism for the Al:Ni = 1:1 composition in SHS regime. According to their work, the reaction starts with Al melting and no solid-state interaction between the reactants occurs. The reaction proceeds through a simple dissolution−precipitation mechanism, with a continuous forming and dissolving of a reaction diffusion layer on the surface of the Ni particles. The formation of the reaction diffusion layer has been shown to be in good agreement with Al− Ni phase diagram. AlNi is the only product phase, and no intermediate reaction occurs. In agreement with other experimental reports,[10] the combustion temperature measured by these authors is above the melting point of Ni but slightly below the melting point of AlNi, and the propagation speed is around 10 mm/s.

However, the propagation speed is strongly dependent on the grain size of the reactants: using much finer particle sizes, Naiborodenko and Itin found wave velocities between 40 and

* To whom correspondence should be addressed. Fax: +39 0382 507575. E-mail: filippo@chifis.unipv.it.

10.1021/jp021821o CCC: $25.00
Published on Web 12/18/2002

130 mm/s. The experimental results depicted for the SHS of powder mixtures by Fan et al.[5] is markedly different from what was observed by other investigators, who studied combustion of Al−Ni foil ensembles[13,14] or by the thermal explosion method.[15] In foil experiments, for instance, the reaction is initiated only by Ni melting and the measured velocities are much higher (up to several m/s, depending on the layer thickness). This has been related to the high density and thermal conductivity of the samples.

In this respect, computer simulation is important as a direct support to the experimental work. In the investigation of the chemical mechanism of SHS processes, the simulation approach provides a tool for exploring the effect of the real process variables, that is determining the trend of the scarce experimentally measurable quantities as a function of the variables that is actually possible to change from experiment to experiment. Numerical simulations based on assumed mechanisms can then be compared to the experiments for assessing or discarding these mechanisms and for suggesting further experiments. In this respect, a computer simulation is not necessarily expected to reproduce exactly the experimental data, a task which typically requires parameters of kinetic nature that are not previously known, that can be determined only after a trustworthy assessment of the mechanism, or else that are impossible to determine independently of an SHS experiment.

The aim of the present work is to describe a particular implementation of a flexible simulation method for investigating the chemical mechanisms of SHS processes and to present its first results. The general guidelines of the method (with application to the SHS between Zr metal and oxygen gas) have been presented in previous papers,[16,17] whereas the chemistry of the model has been rewritten to account for the reactivity in the Al/Ni system, as described in the following section.

2. Computational Model

Thermodynamics. According to the literature,[18,19] the Al/Ni system is characterized by five intermetallic compounds, whose compositions are Al_3Ni, Al_3Ni_2, AlNi, Al_3Ni_5, and $AlNi_3$. Among these, AlNi melts congruently at 1911 K and shows quite a large homogeneity range. $AlNi_3$, Al_3Ni_2, and Al_3Ni_5 have narrower homogeneity ranges and are stable at low temperature. Al_3Ni is, on the contrary, an almost exactly stoichiometric compound and melts incongruently at 1127 K. In the present work, only AlNi has been taken into consideration and has been assumed as a line compound. Accordingly, the assumed phase diagram shows only two eutectic points, one between pure Al and the compound and one between the compound and pure Ni: the former one occurs not much below the melting temperature of the metal (902 K).

Enthalpies, heat capacities, heats of transition (melting) for the pure reactants are taken from literature data,[20] with a suitable modification in order to simplify and speed calculations. Briefly, enthalpies are expressed with a linear dependence from temperature, that is with constant values of heat capacity for each pure phase. The thermodynamic data used in the simulation are as follows:

$$\mathrm{H(Al,s)} = -8344 + 28T \quad \mathrm{J\ mol^{-1}} \qquad T < 902\ \mathrm{K}$$

$$\mathrm{S(Al,s)} = -132 + 28 \ln T \quad \mathrm{J\ mol^{-1}\ K^{-1}} \qquad T < 902\ \mathrm{K}$$

$$\mathrm{Cp(Al,s)} = 28 \quad \mathrm{J\ mol^{-1}\ K^{-1}} \qquad T < 902\ \mathrm{K}$$

$$\mathrm{H(Al,l)} = -1300 + 29T \quad \mathrm{J\ mol^{-1}} \qquad T > 902\ \mathrm{K}$$

$$\mathrm{S(Al,l)} = -130 + 29 \ln T \quad \mathrm{J\ mol^{-1}\ K^{-1}} \qquad T > 902\ \mathrm{K}$$

$$\mathrm{Cp(Al,l)} = 29 \quad \mathrm{J\ mol^{-1}\ K^{-1}} \qquad T > 902\ \mathrm{K}$$

$$\mathrm{H(Ni,s)} = -9834 + 33T \quad \mathrm{J\ mol^{-1}} \qquad T < 1710\ \mathrm{K}$$

$$\mathrm{S(Ni,s)} = -160 + 33 \ln T \quad \mathrm{J\ mol^{-1}\ K^{-1}} \qquad T < 1710\ \mathrm{K}$$

$$\mathrm{Cp(Ni,s)} = 33 \quad \mathrm{J\ mol^{-1}\ K^{-1}} \qquad T < 1710\ \mathrm{K}$$

$$\mathrm{H(Ni,l)} = -900 + 38T \quad \mathrm{J\ mol^{-1}} \qquad T > 1710\ \mathrm{K}$$

$$\mathrm{S(Ni,l)} = -187 + 38 \ln T \quad \mathrm{J\ mol^{-1}\ K^{-1}} \qquad T > 1710\ \mathrm{K}$$

$$\mathrm{Cp(Ni,l)} = 38 \quad \mathrm{J\ mol^{-1}\ K^{-1}} \qquad T > 1710\ \mathrm{K}$$

A similar simplified model for the thermodynamic properties of AlNi has been evaluated along the following guidelines. The thermodynamic functions for liquid phase (Al/ Ni) mixtures are available from literature.[21] From these and from the equilibrium phase diagram, it is possible to evaluate the free energy of the intermetallic compound. Two values have been evaluated at 1406 K (where the equilibrium composition of the liquid phase is assumed as $x_{Ni} = 0.27$ according to experimental information) and at 1911 K, melting point of the compound. In close analogy with what was done for the pure solid reactants, the thermodynamic data for the compound have been written as

$$h(T) = h^* + C_p T \quad \mathrm{J\ mol^{-1}}$$

$$s(T) = s^* + C_p \ln(T) \quad \mathrm{J\ mol^{-1}\ K^{-1}}$$

$$g(T) = h^* + C_p T - T[s^* + C_p \ln(T)] \quad \mathrm{J\ mol^{-1}}$$

where h^*, s^*, and C_p are the quantities to be determined. Using two free energy values, there is one degree of freedom. By (quite arbitrarily) setting the heat capacity to 30 J mol^{-1} K^{-1}, we obtain $h^* = -53\,329$ J mol^{-1}, $s^* = -149.85$ J mol^{-1} K^{-1}, which gives $\Delta H°(298) = -44\,389$ J mol^{-1} and $S°(298) = 21.06$ J mol^{-1} K^{-1} and the adiabatic temperature (for the equi-molar starting mixture) of ~1800 K, that is somewhat below the melting point of the compound. Then, the thermodynamic functions used for the solid intermetallic are

$$H(\mathrm{Al_{0.5}Ni_{0.5}},\mathrm{solid}) = -53329 + 30T \quad \mathrm{J\ mol^{-1}}$$

$$S(\mathrm{Al_{0.5}Ni_{0.5}},\mathrm{solid}) = -149.85 + 30 \ln T \quad \mathrm{J\ mol^{-1}\ K^{-1}}$$

$$Cp(\mathrm{Al_{0.5}Ni_{0.5}},\mathrm{solid}) = 30 \quad \mathrm{J\ mol^{-1}K^{-1}}$$

We stress the fact that these and the above values do not represent an assessment of the binary system; that is, they have not been selected for the purpose of reproducing in the best way the thermodynamics of the system under investigation: the simplifying assumptions (line compound nature of the intermetallic, strongly simplified temperature dependence of the heat capacities of all the solid phases) do not allow to reach this goal. The aim of the model and assumptions, and of the numerical values, are instead to provide a simple but consistent way of reproducing in the simplest way the thermodynamic aspects that are here considered significant: topology of the binary phase diagram, melting points of reactants and product, and an adiabatic temperature slightly lower than the melting point of the compound.

The thermodynamic feasibility of a SHS reaction is most naturally discussed using enthalpy/temperature diagrams. Figure

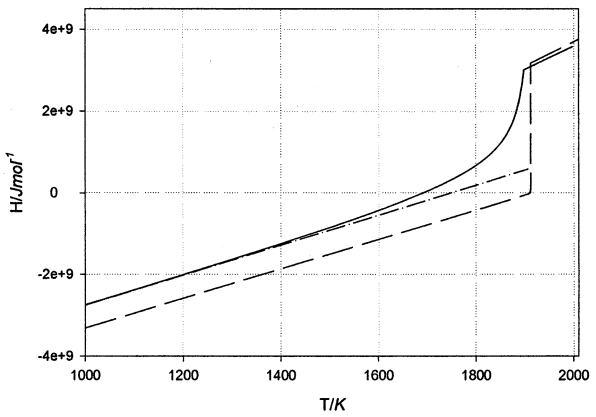

Figure 1. Enthalpy of the system as a function of temperature. The dashed line refers to a composition of 0.49, whereas the continuous line is for a starting Ni molar fraction of 0.45 and the dash−dotted line is an extrapolation to high temperature of the low temperature trend of the continuous line. The underlying thermodynamic data are slightly modified with respect to the values used in the simulation runs to make more clear the significant effect of starting composition on adiabatic temperature.

1 shows such a diagram for two starting compositions. Actually, the underlying thermodynamic data of Figure 1 are slightly modified with respect to those listed above to make clearer a point that is not so obvious but is most significant for the feasibility of the SHS process, that is, the strong dependence of the adiabatic temperature on composition of the starting mixture. As the figure shows, a change from $x = 0.5$ to 0.45 in the molar ratio of the starting mixture lowers by some 250 K the adiabatic temperature. This lowering of the adiabatic temperature can be associated to two logically different but closely related effects: lower overall exothermicity of the reaction and the details of the phase diagram, with the melting of the compound at a lower temperature. The latter effect can be appreciated by comparing the continuous line with the dash−dotted line, which is the linear extrapolation to high temperature of the continuous line and corresponds to what would be expected from a simple stoichiometric evaluation of the amount of compound that can be produced by the reaction. Such a strong influence must be expected for all cases where the adiabatic temperature of the stoichiometric mixture is slightly below the melting point of the compound and is even more important when the adiabatic temperature exactly corresponds to its melting point. Therefore, it must be considered carefully when discussing and comparing experimental results.

Kinetics. To describe the time evolution of an SHS process we rely on a computational method described in previous papers.[16−17] To give here a brief summary, the method is based on the uncoupling between micro- and macrokinetic aspects. The microkinetic treatment describes the behavior of the system at the level of the grains of the solid phases involved in the various phase transformations and chemical reactions. All of the chemistry of the overall SHS process is described at this microkinetic level and can be divided at will into various steps, possibly with several different kinetic laws (mechanisms) for each step, as discussed below.

The macrokinetic treatment deals with the Fourier heat balance equation. The microkinetic variables (temperature and conversion degrees of the various chemical steps, which are only functions of time in the microkinetic treatment) are now taken as continuous functions of both time and space variables and inserted into the Fourier equation, which is solved by a FD (finite differences) algorithm. At each interval of the discrete time slicing, after an upgrade of the temperature by the FD routine, the advancement degrees of the various assumed steps at each space interval are updated by a suitable "chemical" routine, which also calculates the associated amount of energy released or absorbed (q_{chem}), to be in turn inserted into the FD algorithm for the next time interval.

Incidentally, we note that the chemical routine fully encloses the microkinetic aspects of a particular SHS reaction. This is the part of the program that needs to be changed when investigating a novel SHS process, whereas the FD macrokinetic "engine" is left unmodified. On the other side, the organization of the software makes possible to change various aspects of the FD algorithm, leaving unmodified the chemical routine. We plan, for instance, to investigate different ignition processes with a preset heat flux cycle or temperature cycle, to address variants, such as thermal explosion or field assisted SHS, of the usual SHS technique, as well as to insert the chemical model (after its test with the present FD approach) into other more powerful PDE "engines" to investigate aspects that are out of reach of the present program, particularly the extension to 2D and 3D to explore oscillations and instabilities in space and not only in time.

Now, the SHS process

$$\mathrm{Al\ (s) + Ni\ (s) \rightarrow AlNi\ (s)}$$

is described using a one-dimensional model and assuming a starting microstructure made of spherical, equally sized, and uniformly distributed Ni particles embedded in a continuous solid Al pool. The chemical aspect of the problem involves many phase transformations or reactions: (a) melting of the Al reactant; (b) diffusion-controlled dissolution of solid nickel into the molten pool; (c) (possible) melting of the Ni reactant; (d) precipitation and melting of the compound; (e) precipitation of the eutectic mixture of Al + AlNi.

Melting of pure solid aluminum (a), eutectic crystallization (e), and possible melting of nickel (c) are considered only in terms of thermal balance. The assumption is that the kinetics of these steps is controlled only by energy transport, which is accounted for at the macro level: let us say that these processes are treated "without kinetics" at the microkinetic level.

The most important step of the SHS is then the dissolution of solid nickel into the liquid phase, which is at the beginning pure aluminum and gets richer in nickel as the SHS reaction proceeds. For simplicity, the dissolution of nickel is considered here as occurring only after complete melting of aluminum. This process is assumed as controlled by the kinetics of diffusion of the Ni component from the solid/liquid interface into the bulk of liquid. An exact analytic solution for the kinetics of the diffusion-controlled dissolution of a spherical particle into a finite liquid pool is not known. The simplified kinetic law used here comes from the invariant-field approximation of the underlying diffusion equation (also known as the Laplace approximation)[22] and is written as

$$r^2 = r_0^2 - kDt$$

where r is the radius of the particle at a given time, r_0 is its initial value, and

$$k = 2\frac{C_\mathrm{i} - C_\mathrm{m}}{C_\mathrm{s} - C_\mathrm{m}}$$

where C_i is the liquid composition at the precipitate-matrix

interface, C_m is the far-field composition of the liquid alloy and C_s is the reciprocal molar volume of solid Ni.

For the diffusion coefficient (D) an Arrhenius form is used

$$D = D_0 e^{\frac{-E_a}{RT}}$$

where the numerical values for activation energy (E_a) and preexponential term (D_0) have been obtained with a comparison of experimental data from our group[23] and literature data:[11−12]

$$E_a = 76 \text{ kJ mol}^{-1}$$

$$D_0 = 10^{-4} \text{ m}^2 \text{ s}^{-1}$$

As the liquid gets richer in Ni and before complete dissolution of the initial Ni grain, the composition eventually crosses the boundary between the single phase (liquid) and two-phases (liquid/compound) fields, and the deposition of solid compound is thermodynamically allowed. A kinetic hindering of this further reaction step is obviously possible but has not been accounted for in the present chemical model, where its rate is only indirectly controlled (by heat transport) at the macrokinetic level. The reactive dissolution of solid Ni into liquid is presently considered as a single diffusional step, regardless of the fact that the dissolved fraction of original Ni particle goes entirely into the liquid phase or partially goes into the compound phase. The step is algorithmically treated at each time interval by first accounting for diffusion and then adjusting (if and when the phase boundary is eventually reached) the liquid composition and amounts of phases according to the equilibrium composition of the liquid phase at the temperature of the time interval. In either case (with or without compound precipitation), the appropriate heat release (q_{chem}) is evaluated and inserted into the FD coefficients of the Fourier equation for the next time integration step.

Actually, a similar walk of the state of the system along the phase boundary also occurs as a result of the changes in temperature (due to energy transport) after complete dissolution of the Ni reactant, that is when the chemical reaction is already completed. Although the former case describes a reaction step (an out of equilibrium process), the latter case concerns an equilibrium (reversible) process. For consistency reasons and for making easier both implementation of the model and discussion of the results, the latter case is algorithmically treated on the basis of enthalpy balance, analogously to the treatment of the other reversible phase transformations.

The system of partial differential equations to be solved is hence

$$\begin{cases} \dfrac{\partial T}{\partial t} = \dfrac{1}{C}\dfrac{\partial}{\partial x}\left(\chi \dfrac{\partial T}{\partial x}\right) + \dfrac{2\sigma\epsilon(T^4 - T_a^4)}{RC} + \dfrac{\dot{q}_{chem}}{C} \\ \dot{q}_{chem} = f(x,T,t) \end{cases}$$

where C is the heat capacity per unit volume, χ is the thermal conductivity, σ is the Stefan−Boltzmann constant, and ϵ is the emissivity of the external surface of the sample. The Fourier equation for the transport of heat (first equation) has been written for a cylindrical sample of radius R and length L, and dependence of T from other spatial coordinates (y, z) has been neglected. The left side of the equation represents the accumulation of heat, whereas the right side includes the contributions of thermal conductivity, irradiation, and the generation or dissipation of heat due to the chemical reactions or phase transformations.

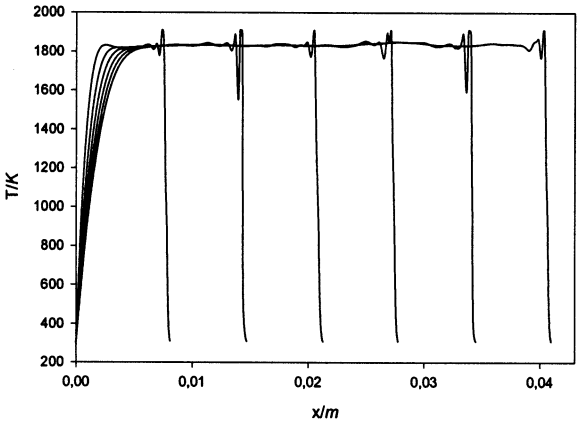

Figure 2. Temperature at different times as a function of position along the sample for a starting Ni composition of 0.49 (mole fraction).

Initial and boundary conditions for Fourier equation are

$$\begin{cases} T(x,t=0) = T_a \ \forall x \in \{0,L\} \\ T(0,t) = f_1(t) \\ T(L,t) = f_2(t) \end{cases}$$

where f_1 and f_2 are given functions: for f_2, we usually take a constant value (T_a = 298 K), while f_1 is a suitable ignition function, hereafter assumed in Gaussian form, where height (maximum ignition temperature), width (time range of ignition) and position (time lag) can be indipendently set. Numerical solutions for the system have been obtained using the finite difference Crank Nicholson scheme.[24]

In the present simulations, the radius of the cylindrical sample (R) has been fixed at 10 mm, the initial radius of the Ni particles (r_0) at 10 μm, the surface emissivity at 0.99, and the thermal conductivity of the heterogeneous mixture has been obtained from that of the constituent phases by a simple linear dependence from composition (this point will be further discussed). Moreover, only starting composition $x < 0.5$ have been considered (x = mole fraction of Ni).

3. Results and Discussion

Figure 2 shows the time evolution of the thermal SHS wave for an almost stoichiometric starting mixture (x = 0.49). As the figure clearly shows, the dynamic behavior of the system is here (mildly) pulsating, with some temperature spikes near the combustion front and an almost uniform and constant plateau at about 1800 K (just below the pertinent adiabatic temperature).

To enlighten the oscillatory behavior of the underlying reaction steps, Figures 3 and 4 show, for the same simulation run and on the same scale but at different times, the space profiles of temperature and of some compositional variables.

Starting from the right side of Figure 3, temperature (dash−dotted line) first increases regularly because of energy transport in the yet unreacted starting mixture and then shows a first knee with a marked decrease of slope at melting of Al (902 K). After this point, nickel starts diffusing in the molten pool: its amount (dotted line) decreases and the molar fraction of Ni in the liquid phase (dashed line) increases.

The onset of precipitation of the solid compound (its amount is given by the continuous line) initially does not significantly affect the temperature profile (dash−dots). However, another knee of temperature profile (now an increase of slope) appears slightly above 1200 K at the position within the sample where (at the selected time) the *rate* of compound deposition reaches its maximum.

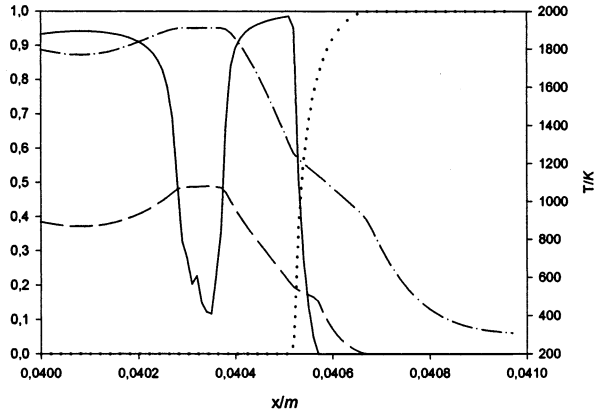

Figure 3. Temperature (dash−dot line, right axis), composition of the liquid phase (Ni mole fraction, dashed line, left axis), and amounts of solid compound (normalized to 1 = stoichiometric amount, continuous line, left axis) and of solid nickel (normalized to 1 = starting quantity, dotted line, left axis) as a function of position within the sample at fixed time. The values correspond to a time when the propagation speed is at its maximum.

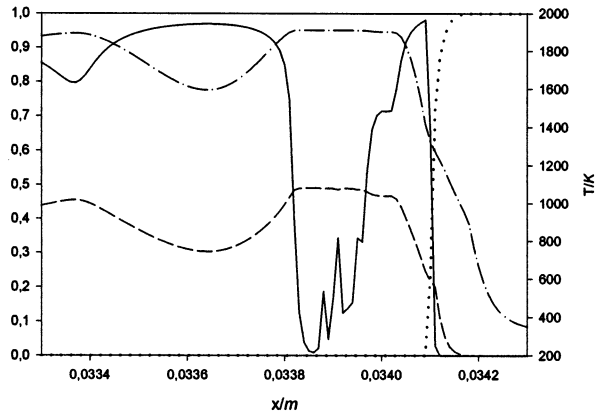

Figure 4. Temperature (dash−dot line, right axis), composition of the liquid phase (dashed line, left axis), and normalized amounts of solid compound (continuous line, left axis) and of solid nickel (dotted line, left axis) as a function of position within the sample at fixed time. The values correspond to a time when the propagation speed is at its minimum.

After complete dissolution of the solid Ni reagent, the temperature profile shows a plateau, which closely mirrors a plateau in liquid composition. In correspondence to these, the system shows a remarkable decrease in the amount of solid compound (continuous line), an effect caused by the attainment of a temperature close to the boundary of the (liquid + solid compound) biphasic region of the phase diagram (for the selected starting composition), which is close to the melting point of the pure compound. All of these features are due to the model which constrains the system to follow the equilibrium conditions.

Finally, some residual oscillations in temperature (dash−dots), liquid composition (dashes), and amount of solid compound (continuous line) can be seen before reaching quite uniform values.

Although the space profiles of Figure 3 are sampled at a time step corresponding to a maximum of the speed of wave propagation, the profiles of Figure 4 correspond to a time step where the wave propagation speed is at a minimum. These profiles clearly show a steeper initial shape of the temperature profile (dash−dots) and wider plateaus of the temperature and liquid composition (dashes) profiles, coupled to larger fluctuations in the amount of solid compound (continuous line), and stronger oscillations in the final parts of the profiles.

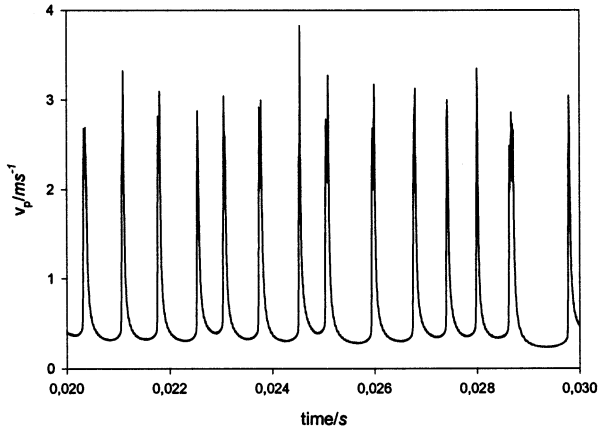

Figure 5. Wave velocity as a function of time with a starting composition = 0.49 (Ni mole fraction) and the thermal conductivities of the bulk phases are used.

The simple pulsating nature of the SHS reaction is clearly shown by the oscillations in time of propagation speed of the overall SHS process, as determined by the time evolution of the thermal wave (Figure 5).

Figures 3−5 are good representatives of the detailed information supplied by the present simulation tool and of its relation with the scarce information given by real experiments, which typically sample the space profiles of the temperature wave (dash−dotted lines of Figures 3 and 4), the time profiles of the wave speed (Figure 5), the dynamic propagation mode, or determine phase compositions and amounts at a narrow range of positions within the sample after a (hopefully faithful) thermal quenching. Although a faithful assessment of the various mechanistic assumptions is eventually given by experiments, the computer simulation provides a tool for probing the consequences of these assumptions and therefore for progressively adjusting our understanding. With respect to analytical methods, the computer simulation makes it possible to explore SHS processes where many different reactive steps are active and can be rate determining under different local conditions, a case where an analytic approach may easily become impracticable.

Within the general guidelines of the present approach it is also fairly easy to make more complex the underlying chemical model to account for available information. In the present model, as said in the previous section, the rate of compound precipitation is treated "without kinetics" at the microlevel, because it is only indirectly controlled by heat transport at the macrolevel. If required, a more specific mechanism and kinetic law, describing a rate of nucleation or a rate of growth or both, can be inserted in the microkinetic aspects of the model. Another useful feature is the possibility of separately exploring physical effects that are coupled in real experiments.

As a matter of fact, the mean propagation speed here obtained (around 0.65 m s^{-1}) is a quite high value with respect to values experimentally determined with SHS on powder compacts but is in reasonable agreement with experiments on samples made of fully densified layers.

As already said in the Introduction, the speed of the SHS wave is about 2 orders of magnitude higher when measured on foil ensembles. In real SHS processes on powder compacts, the compaction pressure or compaction degree of the ensemble of initial reactant grains is indeed the single experimental variable

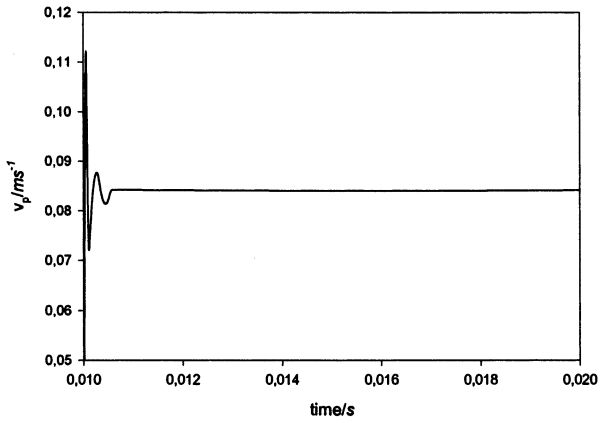

Figure 6. Wave velocity as a function of time with a starting composition = 0.49 (Ni mole fraction) and a fraction $^1/_{70}$ of the thermal conductivities of the bulk phases are used. W m^{-1} K^{-1}. The propagation gets steady as thermal conductivity is lowered.

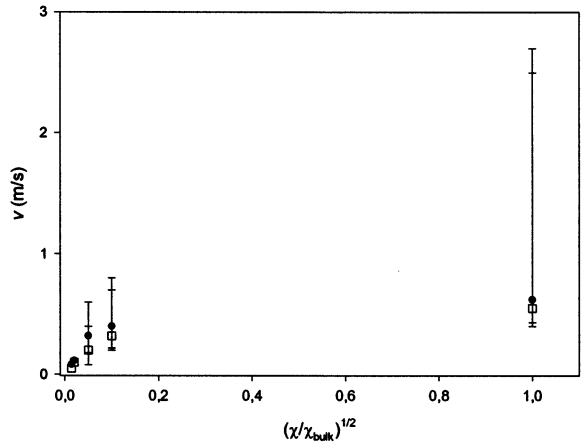

Figure 7. Propagation rate as a function of the square root of thermal conductivity for composition 0.49 (full circles) and 0.46 (empty squares).

that is most difficult to reproduce consistently, and the low reproducibility is well seen by its effects on the macrokinetic parameters.

Although the compaction degree is expected to affect the extensive energy-related quantities (heat of reaction and heat capacities), there are clear indications, on the other side, that the effective thermal conductivity of a powder mixture is drastically reduced with respect to the corresponding fully densified bodies. Actually, Miura et al.[25] have experimentally shown that thermal conductivity varies with compaction degree, and pointed out that the thermal conductivity of a powder Al + Ni mixture can be 2 orders of magnitude lower than its bulk value. For this reason, various values for thermal conductivity have been considered down to $^1/_{70}$ of its bulk value, which actually represents the minimum value for ignition of the reaction under study.

With computer simulation, it is quite easy to uncouple the two effects of compaction by independently setting the values of sample density (that is the amount per unit volume of both reactants) and the sample thermal conductivity.

Naively, one may expect a parallel trend of propagation speeds and combustion modes, in the sense that slower propagation speeds correspond to propagation modes "closer" to extinction (that is to some form of unsteady propagation) and, on the contrary, faster propagation speeds correspond to stationary propagation mode (or propagation modes "closer" to stability).

This naive thinking is in agreement with some theoretical and numerical studies[26,27] and corresponds to the results of our previous simulation studies of the Zr + O_2 SHS, where a whole sequence of different unsteady modes are found between the domains of steady combustion and extinction: by progressively changing the SHS process parameters to less exothermic conditions, the steady combustion turns first into a simple pulsating regime (a simple oscillation in time), then into a more complex pulsating regime (with multiple oscillations in time), then into chaotic behavior, and finally into extinction, and *correspondingly lower SHS speeds* are obtained.

With the present simulations, the effect of sample conductivity can be explored by setting different values without changing the amount of reactants per unit volume. The result is that, with decreasing the conductivity values, the mean propagation speed decreases, but dynamic behaviors "*closer to steady propagation*" are progressively obtained. The trend is well indicated by Figure 6 which reports the time profile of the wave speed for a simulation run with the same parameters of Figure 5 but a 70 times lower thermal conductivity (as said, this is the lowest conductivity at which the SHS actually shows ignition when the selected values of the other simulation parameters are kept fixed). The same plot and the space profile of temperature (not shown) clearly indicate steady propagation.

This counter-intuitive behavior indeed corresponds to some experimental results on SHS of very exothermic materials. The indication (very broadly speaking) that a faster SHS reaction couples to the onset of pulsating propagation is also in agreement with the theoretical analysis by Makino.[28] In this respect, an important indication by this Author concerns the different effects of process parameters on transversal and longitudinal instabilities. The present simulations account only for the latter kind, and a more complete comparison of our simulation results with the above analytical treatment will be done after the planned extension of our model to 3D.

On the other side, the effect of reaction exothermicity can be explored by setting progressively lower molar amounts (of both reactants) per unit volume leaving unmodified (to its bulk value) the thermal conductivity. Then, faster waves are found with less dense reactants, this showing that the effects of the reaction exothermicity and thermal conductivity on the speed of an SHS reaction are opposite to each other (but the latter one is largely predominant).

The wave velocity obtained with lower conductivity indeed shows a comfortable agreement with typical results of experiments on powder compacts. For instance, a typical value of wave speed obtained using $^1/_{70}$ of the bulk value of thermal conductivity for a composition close to 0.5 in molar fraction is about 0.08 ms^{-1} (see also Figure 7).

Conclusions

The chemical model here assumed describes in a comprehensive way the overall SHS reaction of an intermetallic compound by considering several elemental steps such as melting of the reactant Al, diffusion-controlled dissolution of solid nickel into the molten pool, (possible) melting of the Ni reactant, precipitation and melting of the compound, and precipitation of the eutectic mixture of Al + AlNi.

Simplifying assumptions at the thermodynamic level are that a single binary compound is considered, that it is taken as a line compound, and that the heat capacities of the pure phases are taken as temperature independent, whereas mixture proper-

ties of the liquid phase are modeled by directly using accurate experimental calorimetric determinations.[21]

Simplifying assumptions at the kinetic level are that melting of pure aluminum (and possibly pure nickel), eutectic crystallization, and compound deposition under equilibrium conditions are computed only in terms of energy balance, so that their kinetics is controlled indirectly only by energy transport. An explicit kinetic law is presently assumed only for the out-of-equilibrium dissolution of nickel in molten aluminum, which is described by a diffusion controlled mechanism. Kinetic laws for nucleation or growth of solid phases, however, can be easily added to the chemical model if required.

More generally, a further simplifying assumption concerns the 1D nature of the model. To overcome this limitation, we plan to replace the present FD "engine" with methods suitable for 3D models. A useful outcome of the general approach described here is that the chemical description at the microkinetic level and the macrokinetic description concerning Fourier's law of heat balance are logically and algorithmically uncoupled, so that every one of them can be changed independently. On one side, the chemical routines can be refined without changing the algorithms for solving the PDE equations, and on the other side, these algorithms can be improved leaving unmodified the already tested chemical routines.

The first results show that when bulk values of the thermal conductivity of the reacting mixture are used the reaction propagates under mildly oscillating conditions and with a speed that is in reasonable agreement with SHS experiments on film samples.

When remarkably lower values (about 70 times lower) for the thermal conductivity are set, almost steady conditions with constant wave velocity are obtained, and the velocity values are close to those experimentally reported for SHS on powder mixtures. Also, the order of magnitude of reduction of thermal conductivity required to achieve this result is in agreement with experimental determination of the thermal conductivity of green compacts.

References and Notes

(1) Moore, J. J.; Feng, H. J. *Prog. Mater. Sci.* **1995**, *39*, 243.
(2) Moore, J. J.; Feng, H. J. *Prog. Mater. Sci.* **1995**, *39*, 275.
(3) Munir, Z. A.; Anselmi-Tamburini, U. *Mater. Sci. Rep.* **1989**, *3*, 277.
(4) Munir, Z. A.; Odink, D. In *Metallurgical Processes of the Early Twenty-First Century*; Sohn, H. Y., Ed.; TMS: Warrendale, PA, 1994; p 167.
(5) Fan, Q.; Chai, H.; Jin, Z. *Intermetallics* **2001**, *9*, 602.
(6) Anselmi-Tamburini, U.; Campari, G.; Spinolo, G. *Rev. Sci. Instrum.* **1995**, *66*, 5006.
(7) Charlot, F.; Bernard, F.; Gaffet, E.; Klein, D.; Niepce, J. C. *Acta Mater.* **1999**, *47*, 619.
(8) Riley, D. P.; Kisi, E. H.; Hansen, T. C.; Hewat, A. W. *J. Am. Ceram. Soc.* **2002**, *85*, 2417.
(9) Merzhanov, A. G.; Borovinskaya, I. P.; Ponomarev, V. I.; Khomenko, I. O.; Zanevskii, Yu. V.; Chernenko, S. P.; Smykov, L. P.; Cheremukhina, G. A. *Doklady Akademii Nauk.* **1993**, *328*, 72.
(10) Naiborodenko, Yu. S.; Itin, V. I. *Sov. Phys. J.* **1973**, *16*, 1507.
(11) Naiborodenko, Yu. S.; Itin, V. I. *Combust. Explos. Shock Wave* **1975**, *2*, 343.
(12) Naiborodenko, Yu. S.; Itin, V. I. *Combust. Explos. Shock Wave* **1975**, *2*, 734.
(13) Anselmi-Tamburini, U.; Munir, Z. A. *J. Appl. Phys.* **1989**, *66*, 5039.
(14) Dyer, T. S.; Munir, Z. A. *Metall. Mater. Trans. B* **1995**, *26*, 603.
(15) Philpot, K. A.; Munir, Z. A.; Holt, J. B. *J. Mater. Sci.* **1987**, *22*, 159.
(16) Arimondi, M.; Anselmi-Tamburini, U.; Gobetti, A.; Munir, Z. A.; Spinolo, G. *J. Phys. Chem. B* **1997**, *101*, 8059.
(17) Maglia, F.; Anselmi-Tamburini, U.; Gennari, S.; Spinolo, G. *Phys. Chem. Chem. Phys.* **2001**, *3*, 489.
(18) Murray, J.; Peruzzi, A.; Abriata, J. P. *J. Phase Equilib.* **1992**, *13*, 277.
(19) Hansen, M.; Anderko, K. In *Metallurgy and Metallurgical Engineering Series: Constitution of Binary Alloys*; Mehl, R. F., Bever, M. B., Eds.; MacGraw-Hill Book Company: New York, 1958.
(20) *Handbook of Chemistry and Physics*, 67th ed.; Weast, R. C., Ed.; The Chemical Rubber Co.: Boca Raton, FL, 1986−1987.
(21) Grigorovitch, K. V.; Krylov, A. S. *Thermochim. Acta* **1998**, *314*, 255.
(22) Aaron, H. B.; Fainstein, D.; Kotler, G. B. *J. Appl. Phys.* **1970**, *41*, 4404.
(23) Milanese, C. Ph.D. Thesis, Università di Pavia, Pavia, Italy, 2001.
(24) Lapidus, L.; Pinder, G. In *Numerical Solution of Partial Differential Equations in Science and Engineering*; J. Wiley & Sons: New York 1982.
(25) Miura, S.; Terada, Y.; Suzuki, T.; Liu, C. T.; Mishima, Y. *Intermetallics* **2000**, *8*, 151.
(26) Weber, R. O.; Mercer, G. N.; Sidhu, H. S.; Gray, B. F. *Proc. R. Soc. London A* **1997**, *453*, 1105.
(27) Weber, R. O.; Mercer, G. N.; Sidhu, H. S. *Proc. R. Soc. London A* **1998**, *454*, 2015.
(28) Makino, A. *Prog. Energ. Combust.* **2001**, *27*, 1.